

ARTICLE TYPE**Identification of additional young nearby runaway stars based on Gaia data release 2 observations and the lithium test[†]**Richard Bischoff*¹ | Markus Mugrauer¹ | Guillermo Torres² | Michael Geymeier¹ | Ralph Neuhäuser¹ | Wolfgang Stenglein¹ | Kai-Uwe Michel¹¹Astrophysikalisches Institut und
Universitäts-Sternwarte Jena,
Schillergäßchen 2, 07745 Jena, Germany
²Center for Astrophysics | Harvard &
Smithsonian, 60 Garden Street, Cambridge
MA 02138, United States of America**Correspondence***R. Bischoff, Astrophysikalisches Institut
und Universitäts-Sternwarte Jena,
Schillergäßchen 2, 07745 Jena, Germany
Email: richard.bischoff@uni-jena.de**Funding Information**

NE 515/58-1. MU 2695/27-1.

Runaway stars are characterised by their remarkably high space velocities, and the study of their formation mechanisms has attracted considerable interest. Young, nearby runaway stars are the most favorable for identifying their place of origin, and for searching for possible associated objects such as neutron stars.

Usually the research field of runaway stars focuses on O- and B-type stars, because these objects are better detectable at larger distances than late-type stars. Early-type runaway stars have the advantage, that they evolve faster and can therefore better be confirmed to be young. In contrast to this, the catalogue of *Young runaway stars within 3 kpc* by Tetzlaff, Neuhäuser, & Hohle (2011) contains also stars of spectral type A and later. The objects in this catalogue were originally classified as young (≤ 50 Myr) runaway stars by using *Hipparcos* data to estimate the ages from their location in the Hertzsprung-Russell diagram and evolutionary models.

In this article, we redetermine and/or constrain their ages not only by using the more precise second data release of the *Gaia* mission, but also by measuring the equivalent width of the lithium (6708 Å) line, which is a youth indicator. Therefore, we searched for lithium absorption in the spectra of 51 target stars, taken at the University Observatory Jena between March and September 2020 with the Échelle spectrograph FLECHAS, and within additional TRES-spectra from the Fred L. Whipple Observatory. The main part of this campaign with its 308 reduced spectra, accessible at VizieR, was already published. In this work, which is the continuation and completion of the in 2015 initiated observing campaign, we found three additional young runaway star candidates.

KEYWORDS:

stars: HRD, fundamental parameters; methods: observational, data analysis; techniques: spectroscopic; astronomical databases: catalogues

1 | INTRODUCTION

Runaway stars can result from gravitational interactions in dense stellar clusters (Poveda, Ruiz, & Allen, 1967) or from a supernova explosion in a binary system (Blaauw, 1961).

[†]Based on observations obtained with telescopes of the University Observatory Jena, which is operated by the Astrophysical Institute of the Friedrich-Schiller University, and telescopes of the Fred L. Whipple Observatory, which is operated by the Harvard-Smithsonian Center for Astrophysics Cambridge MA.

In both cases the ejected stars move on with higher velocities compared to typical field stars. Runaway stars can be traced back to their birth place by considering the influence of the Galactic potential. The correctness of those calculations depends mainly on the time since the ejection and will be even more challenging after several Myr. Credible runaway stars, that originated e.g. from the explosion in a binary system, should not be older than about 50 Myr (including the lifetime of the progenitor star until the supernova).

In 2011 the catalogue of *Young runaway stars within 3 kpc*¹ was published by Tetzlaff et al., which contains not only O- and B-type stars, but also every type of star with a peculiar space velocity $v_{\text{pec}} > 28$ km/s. These objects were identified within a combined analysis of spatial, tangential and radial velocities, measured by the *Hipparcos* satellite (Perryman et al., 1997). Furthermore, their ages were derived by comparing luminosity and effective temperature to different evolutionary models.

However, these age estimations can be improved and/or constrained with the more accurate second data release (Gaia Collaboration et al., 2018) of the *Gaia* mission (*Gaia* DR2) of the European Space Agency. Additionally, we searched for another youth indicator, namely the absorption line of the lithium doublet at 6708 Å based on Neuhäuser (1997), within our spectroscopic observing program for selected stars from the catalogue by Tetzlaff et al.. This observing program started in 2015 and the first results were already published in Bischoff, Mugrauer, Torres, et al. (2020). The remaining targets of this project are presented and discussed in this article.

In section 2, we describe the sample selection, spectroscopic observations and data reduction. In section 3, we characterise the physical properties of our targets based on their *Gaia* DR2 data and in section 4 we explain the measurements of the Li (6708 Å) line in all taken spectra. Section 5 contains the age estimation of the dwarf stars. Finally, all results are discussed in section 6 and we draw conclusions in section 7.

2 | SAMPLE SELECTION, OBSERVATIONS AND DATA REDUCTION

Our sample was selected from the catalogue by Tetzlaff et al. (2011). These targets had to be brighter than $V \leq 8.5$ mag in order to record spectra with sufficiently high signal-to-noise-ratio (SNR) > 50 within integration times of a few minutes. Furthermore, their declination angle had to be $Dec > -14^\circ$ so that they can be observed at air masses $X < 2.4$ from Jena. As mentioned in Bischoff, Mugrauer, Torres, et al. (2020), in total 460 stars were identified that fulfill these conditions and 308 of them were already observed and published. However, the remaining list of 152 stars could be further shortened

with a rough analysis by using data from *Gaia* DR2 and the catalogue of Bailer-Jones, Rybizki, Fouesneau, Mantelet, & Andrae (2018) to rule out most of the giants. This results in a target list that contains 51 stars, which were observed with the fibre-linked Échelle spectrograph FLECHAS (Mugrauer, Avila, & Guirao, 2014) and processed in the following.

Our spectra were taken with FLECHAS, operated at the Nasmyth-focus of the 90 cm-telescope ($f/D = 15$) of the University Observatory Jena (Pfau, 1984). The observations, that include 153 spectra with a total integration time of 25.75 h, were carried out between March and September 2020.

All spectra were recorded with the 1x1 binning mode of the spectrograph FLECHAS, using individual detector integration times in the range between 150 s and 1200 s dependent on the target brightness. The instrument has a resolving power of $R \approx 9,300$ and covers a spectral range from 3900 Å to 8100 Å within 29 orders (Mugrauer et al., 2014). Three spectra per target were always taken to remove cosmics and to reach a sufficiently high SNR, which was measured in all fully reduced spectra at $\lambda = 6700$ Å, which is the centre of the spectral order with the Li (6708 Å) line. On average SNR = 101 is reached in the FLECHAS spectra of our targets, with range from 50 for HIP 30030 to 201 for HIP 19587. Further details are given in the observation log in Table A1.

Three flat-field frames of a tungsten lamp and three spectra of a thorium-argon (ThAr) lamp are recorded immediately before the observation of each target for calibration purposes. Each calibration file has an individual integration time of 5 s. About 700 detected emission lines are available in the ThAr spectra for wavelength calibration. The long-term stability of the wavelength calibration of FLECHAS was confirmed in studies by Irrgang, Desphande, Moehler, Mugrauer, & Janousch (2016), Bischoff et al. (2017), Heyne et al. (2020) and Bischoff, Mugrauer, Lux, et al. (2020). Additionally, for the dark subtraction, three dark frames for all used integration times were taken in every observing night. An overscan region is always read out to measure and later correct the bias level. The FLECHAS detector has a typical read-noise of about $11 e^-$ and the gain is $1.3 e^-/\text{ADU}$. The FLECHAS CCD-sensor and the whole instrument is described in detail in Mugrauer et al. (2014).

The observations were reduced with a dedicated pipeline for FLECHAS, developed at the Astrophysical Institute Jena, which includes dark and bias subtraction, flat-fielding, extraction and wavelength calibration of the individual spectral orders. Furthermore, including the final averaging and normalisation of the spectra (Mugrauer et al., 2014).

As part of a separate long-term spectroscopic monitoring program to measure radial velocities and discover binary systems in another sample of runaway stars from Tetzlaff et al. (2011), HIP 2710 and HIP 12297 were also observed between

¹<http://cdsarc.u-strasbg.fr/viz-bin/cat/J/MNRAS/410/190>

September 2013 and March 2017 with the Tillinghast Reflector Echelle Spectrograph TRES (Fűrész, 2008; Szentgyorgyi & Fűrész, 2007). The spectrograph is attached to the 1.5 m Tillinghast reflector at the Fred L. Whipple Observatory on Mount Hopkins (Arizona, USA). This bench-mounted, fibered instrument generates spectra at a resolving power of $R \approx 44,000$ that cover the wavelength region between 3800 \AA and 9100 \AA in 51 orders. Exposure times ranged from 60 s to 250 s, depending on brightness and weather conditions. Exposures of a ThAr lamp were taken before and after each science frame, and the observations were also reduced with a dedicated pipeline, which follows the procedure described in Fűrész (2008).

3 | TARGET CHARACTERISATION WITH GAIA DR2 DATA

The detailed characterisation of our targets in this article focusses mainly on data from the *Gaia* DR2. We considered only gold flag photometry (as described by Andrae et al. 2018) entries from the *Gaia* DR2. The apparent brightness in the *G*-band for each target was corrected according to the brightness relations in Maíz Apellániz & Weiler (2018) and taking into account the new defined transmission profiles for the *Gaia* filters from Weiler (2018). We did not use the estimates for the *G*-band extinction in *Gaia* DR2, because they were not available for 16 targets of our sample and sometimes they were significantly overestimated, e.g. in the case of HIP 56770, an extinction of $A_G = 0.995^{+0.188}_{-0.314}$ mag seems unrealistic, given its distance of 47.8 ± 0.5 pc from Bailer-Jones et al. (2018). Therefore, we take extinctions in the *V*-band from the catalogue of Gontcharov & Mosenkov (2017) instead and convert these values with relations from Wang & Chen (2019) to *G*-band extinctions.

Based on apparent brightness G and extinction A_G in the *G*-band, together with the distances d from Bailer-Jones et al. (2018), we calculated the absolute *G*-band brightness M_G . The used values and results are presented in Table A3. Additionally, we list effective temperatures T_{eff} , stellar radii R and luminosities L of our targets, if available and the target was not a spectroscopic binary.

We show the distance distribution of our targets in Figure 1. It has a median distance of about 75.4 pc. The individual distances range between $22.1^{+0.1}_{-0.1}$ pc (HIP 19855) and 676^{+2027}_{-290} pc (HIP 113811).

However, not all needed parameters were available in *Gaia* DR2, Gontcharov & Mosenkov (2017) and Bailer-Jones et al. (2018) for our complete target sample. HIP 57529, HIP 106053, HIP 113811 and HIP 115906 were missing distance information and therefore, we had to calculate it from

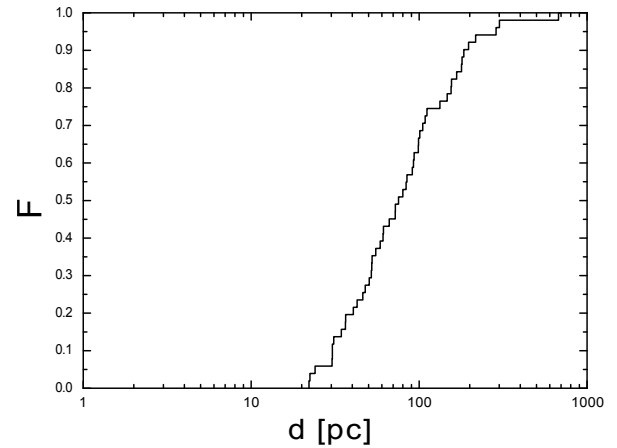


FIGURE 1 The cumulative distribution function of the distances of our sample.

the *Hipparcos* parallax (van Leeuwen, 2007) instead. For the same four targets, we converted the apparent magnitude of the *Hipparcos* system H_p and the $V - I$ magnitudes, provided by the *Hipparcos* catalogue (Perryman et al., 1997), into the *G*-band with the relations by Evans et al. (2018). Their T_{eff} were derived from their *Hipparcos* spectral type (SpT) with the corresponding SpT- $\log(T_{\text{eff}})$ -relations by Damiani et al. (2016). HIP 113811 had also no entry in the extinction catalogue of Gontcharov & Mosenkov (2017). Therefore, we used the reddening $E(g - r)$ from Green, Schlafly, Zucker, Speagle, & Finkbeiner (2019), which was transformed into A_r with the relation given there and afterwards into A_G (Wang & Chen, 2019).

We searched for multiplicity within our sample in the *9th Catalogue of Spectroscopic Binary Orbits* (Pourbaix et al., 2004) to correct their absolute brightness. In the case of a double-lined spectroscopic binary, we took the mass ratio of the secondary and the primary component and converted it into a luminosity ratio via $L \propto M^{4.5}$, which is applicable for stellar masses between $2 M_{\odot}$ and $0.5 M_{\odot}$ (Salaris & Cassisi, 2005), suitable for our sample of spectral types ranging between A7 and K2. The luminosity ratios were then used to determine how much brighter is the binary in comparison to a single source. We assumed that the brightness difference between the secondary and the primary is at least 1 mag for the single-lined binaries, if no further information about mass ratios or the systems were available. It follows that those systems could be up to ~ 0.364 mag brighter than a corresponding single star. The identified spectroscopic binaries and their mass ratios are listed in Table 1.

Our targets are illustrated in a Hertzsprung-Russell-Diagram (HRD) in Figure 2. For example, HIP 113811 ($M_G = -1.891^{+1.275}_{-3.070}$ mag) and

TABLE 1 The spectroscopic binary stars within our target sample. We list their mass ratio M_2/M_1 , if available, and the corresponding reference.

Target	M_2/M_1	ref.
HIP 5081	0.902 ± 0.009	a
HIP 22524	-	
HIP 26690	0.938 ± 0.049	b
HIP 64312	0.729 ± 0.006	c
HIP 71631	0.556 ± 0.127	d
HIP 82798	-	
HIP 112821	-	
HIP 114379	0.973 ± 0.001	e

a Griffin (2001)

b Nordstrom, Stefanik, Latham, & Andersen (1997)

c Escorza et al. (2019)

d König, Guenther, Woitas, & Hatzes (2005)

e Fekel, Henry, & Tomkin (2017)

HIP 115906 ($M_G = -1.754^{+0.459}_{-0.531}$ mag) can be excluded as possible young runaway stars, because they are far too bright for their given T_{eff} to be dwarf stars and are clearly located on the giant branch. Typical M_G - T_{eff} -relations for dwarf stars are given in Pecaut & Mamajek (2013)² and Baraffe, Homeier, Allard, & Chabrier (2015)³. However, it is not always easy to decide, based on their location in the HRD alone, whether an object is either a pre-main-sequence star or it has already left the main-sequence. Therefore, we studied their listed surface gravities in the *StarHorse* catalogue (Anders et al., 2019) and if the given range of $\log(g[\text{cm/s}^2]) \gtrsim 3.8$, the target was classified as dwarf star.

To identify the young stars among the dwarfs, further analysis is needed.

4 | LI (6708 Å) EQUIVALENT WIDTH MEASUREMENTS AND ABUNDANCES

The Ca (6718 Å) line was used to correct the doppler shift in every spectrum, adopting $\lambda_0 = 6717.685$ Å as laboratory wavelength as listed in the ILLSS catalogue (Coluzzi, 1993), because it is the most prominent spectral line nearby Li (6708 Å), and is also detected in the same spectral order.

We measured the equivalent width via a direct integration of the line profiles in the reduced spectra by using the IRAF

(Tody, 1993) task `splot` as explained in Bischoff, Mugrauer, Torres, et al. (2020).

The equivalent widths of the Li (6708 Å) line of all targets are given in Table A2. Furthermore, in appendix *Dwarf stars with significant lithium detection* and *Sub-giant/giant stars with significant lithium detection*, we illustrate all FLECHAS spectra that show a significant detection, that means $EW_{\text{Li}} \geq 3 \cdot \sigma EW_{\text{Li}}$. All spectra are sorted by their spectral type according to SpT- $\log(T_{\text{eff}})$ -relations from Damiani et al. (2016). The uncertainty of the spectral classification is about two sub-classes. In additional TRES-spectra of HIP 2710 and HIP 12297, we searched for lithium as described above. The measured average equivalent width from the four spectra of HIP 2710 is $EW_{\text{Li}} = (43 \pm 7)$ mÅ. In the case of HIP 12297, none of the 24 spectra showed a significant Li (6708 Å) line. These results are consistent with the measurements from FLECHAS.

Our equivalent widths measurements of the identified dwarf stars with significant lithium detection were converted into abundances by using curves of growth from Soderblom et al. (1993), that are based on an abundance scale of $\log_{10}(N)_{\text{H}} = 12$ and we assigned the best matching values of $\log_{10}(EW)$ and T_{eff} (Table 2 in Soderblom et al. 1993) to those of our sample. Indeed, some of our T_{eff} values were outside the covered range of Soderblom et al. (1993). Therefore, we fit quadratic polynomials as a function of T_{eff} for constant values of $\log_{10}(EW)$. The results of this conversion are presented in Table 2.

5 | AGE ESTIMATION

We can constrain the ages of our identified dwarf stars with further isochrones. The isochrones in Figure 3 were calculated with models of Bressan et al. (2012) for metallicity $Z = 0.0152$. Assuming solar metallicity is justified, because all dwarfs exhibit an average metallicity of $[M/H] = 0.09$ with a standard deviation of 0.13 dex. This estimate is based on a compilation of metallicities for our stars from the *VizieR* database (Ochsenbein, Bauer, & Marcout, 2000), taken from the catalogues by Brewer, Fischer, Valenti, & Piskunov (2016), Casagrande et al. (2011), Casamiquela et al. (2020), Franchini, Morossi, di Marcantonio, Malagnini, & Chavez (2014), Gray, Corbally, Garrison, McFadden, & Robinson (2003), Gray et al. (2006), Kunder et al. (2017), Luck (2017), Mann, Brewer, Gaidos, Lépine, & Hilton (2013), Marsden et al. (2014), Petigura & Marcy (2011), Stassun et al. (2019) and Valenti & Fischer (2005). The influence of the metallicity scatter is shown in Figure 4. Here, we show as an example the 50 Myr isochrone. The differences between different metallicities are smaller or

²https://www.pas.rochester.edu/~emamajek/EEM_dwarf_UBVIJHK_colors_Teff.txt

³<http://perso.ens-lyon.fr/isabelle.baraffe/BHAC15dir/>

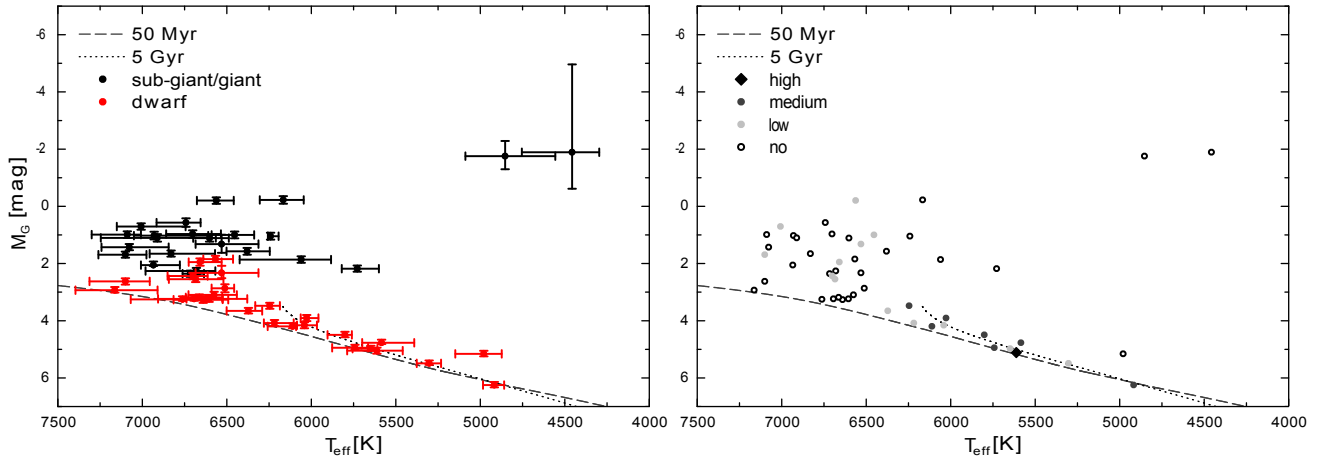


FIGURE 2 Hertzsprung-Russell diagram with all 51 observed targets. On the **left**, we show sub-giant/giant stars marked with full black dots and dwarf stars with full red dots. On the **right**, the targets are characterised by the measured equivalent width of the Li (6708 Å) line: Targets with $EW_{\text{Li}} < 3 \cdot \sigma EW_{\text{Li}}$ have *no* significant lithium detection, while objects with $EW_{\text{Li}} \geq 3 \cdot \sigma EW_{\text{Li}}$ and $EW_{\text{Li}} < 100 \text{ mÅ}$ are ranked as *low*, $100 \text{ mÅ} \leq EW_{\text{Li}} < 200 \text{ mÅ}$ as *medium* and $EW_{\text{Li}} \geq 200 \text{ mÅ}$ as *high*. We have also plotted the PARSEC isochrones (Bressan et al., 2012) for 50 Myr and 5 Gyr with solar metallicity $Z = 0.0152$ in both distributions.

TABLE 2 The classified dwarf stars with their identification numbers as shown in Figure 2, with their effective temperatures T_{eff} from *Gaia* DR2 and the measured equivalent widths of the Li (6708 Å) line EW_{Li} . We list only targets with significant lithium detection. The abundances $\log_{10}(N_{\text{Li}})$ based on Soderblom et al. (1993) are given in the last column.

id. nr.	Target	T_{eff} [K]	EW_{Li} [mÅ]	$\log(N_{\text{Li}})$
1	HIP 28469	6701^{+150}_{-87}	61 ± 12	$3.196^{+0.072}_{-0.318}$
2	HIP 113174	6684^{+159}_{-164}	57 ± 11	$3.135^{+0.133}_{-0.318}$
3	HIP 26690	6659^{+67}_{-128}	66 ± 15	$3.196^{+0.143}_{-0.318}$
4	HIP 2710	6372^{+129}_{-81}	36 ± 12	$2.519^{+0.359}_{-0.152}$
5	HIP 22524	6246^{+86}_{-60}	119 ± 12	$3.260^{+0.090}_{-0.090}$
6	HIP 54531	6218^{+63}_{-114}	85 ± 14	$3.011^{+0.079}_{-0.138}$
7	HIP 51386	6111^{+147}_{-21}	120 ± 11	$3.043^{+0.217}_{-0.087}$
8	HIP 44212	6041^{+44}_{-74}	64 ± 13	$2.593^{+0.136}_{-0.120}$
9	HIP 30030	6027^{+36}_{-69}	190 ± 24	$3.517^{+0.177}_{-0.271}$
10	HIP 114385	5801^{+103}_{-41}	111 ± 10	$2.726^{+0.317}_{-0.082}$
11	HIP 115527	5742^{+135}_{-78}	126 ± 13	$2.808^{+0.332}_{-0.082}$
12	HIP 19855	5648^{+108}_{-39}	71 ± 12	$2.432^{+0.069}_{-0.372}$
13	HIP 16563	5612^{+176}_{-153}	254 ± 14	$3.367^{+0.522}_{-0.522}$
14	HIP 71631	5584^{+115}_{-193}	197 ± 13	$3.000^{+0.271}_{-0.132}$
15	HIP 7576	5303^{+73}_{-71}	114 ± 12	$2.196^{+0.361}_{-0.073}$
16	HIP 40774	4917^{+67}_{-58}	119 ± 12	$1.980^{+0.400}_{-0.400}$

at least comparable with the uncertainties of effective temperature or absolute brightness. Hence, they do not effect the age estimation significantly.

However, we have to consider that many of our dwarf stars are consistent with more than one isochrone within their uncertainties in Figure 3, especially if they are matching one of the Gyr isochrones. For that reason, the estimated ages based on the location in the HRD in Table 3, are sometimes only listed with lower limits. Additional information, as explained in the following, are necessary to identify and/or further constrain the young stars among our targets.

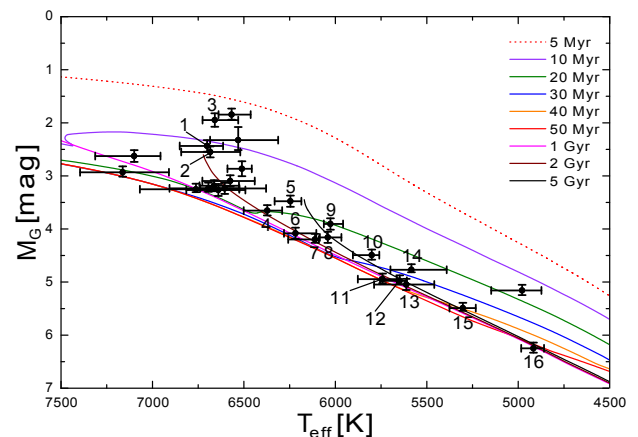


FIGURE 3 The dwarf stars of our sample are illustrated in the Hertzsprung-Russell diagram with different isochrones, using the stellar evolutionary models of Bressan et al. (2012) for solar metallicity $Z = 0.0152$.

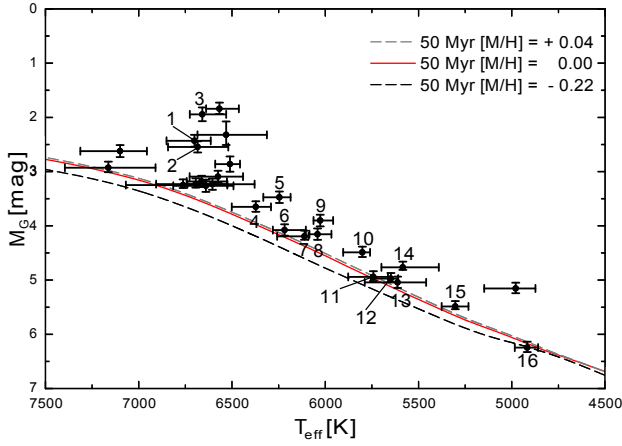


FIGURE 4 The dwarf stars of our sample plotted in the Hertzsprung-Russell diagram with 50 Myr isochrones for different metallicities $[M/H]$ using the stellar evolutionary models of Bressan et al. (2012).

We compared all dwarf stars with significant lithium detection in their spectra to distributions of stellar clusters with known ages, as illustrated in Figure 5. The curves are polynomial fits for observed average equivalent width measurements dependent on T_{eff} (cluster data and fits from E. Mamajek, priv. communication). E. Mamajek’s original plot is available online⁴.

The age errors for this method appear to be 10% – 20%, as stated by Soderblom, Hillenbrand, Jeffries, Mamajek, & Naylor (2014), and the detection of lithium in a low-mass star with known effective temperature can give an upper limit to its age. HIP 22524 (#5 in Table 3 and Figure 5) is only consistent with the 50 Myr curve and within its uncertainties it reaches clearly the area for stars that are younger than 50 Myr. Hence, its assigned age is ≤ 50 Myr. HIP 51386 (#7) and HIP 71631 (#14) fit with more than one age curve and are also consistent with ages below 50 Myr within their uncertainties. Therefore, they were considered to be $\leq 50 \dots 120$ Myr and $\leq 50 \dots 90$ Myr, respectively.

HIP 30030 (#9) and HIP 16563 (#13) should be handled with care, because as stated by Soderblom et al. (2014) the lithium method does not give reliable age estimations below 20 Myr. For that reason, these stars were classified to have an age of < 50 Myr. Furthermore, for $T_{\text{eff}} > 6300$ K the < 5 Myr age curve in Figure 5 is an extrapolation, because in this range no stars with lithium and the corresponding age were observed.

The remaining dwarfs with a significant detected Li (6708 Å) line cross more than one age curve in Figure 5. Their age estimation was encircled by the youngest age curve

and the oldest age curve, that were hit within their uncertainties. For example, HIP 19855 (#12) matches the curves for 500 Myr and 625 Myr and therefore, it was estimated to have an age of 500 to 625 Myr. The age estimations for the others stars are given in the corresponding column of Table 3.

HIP 40774 (#16) is about 175 Myr old, because it only fit with those age curve.

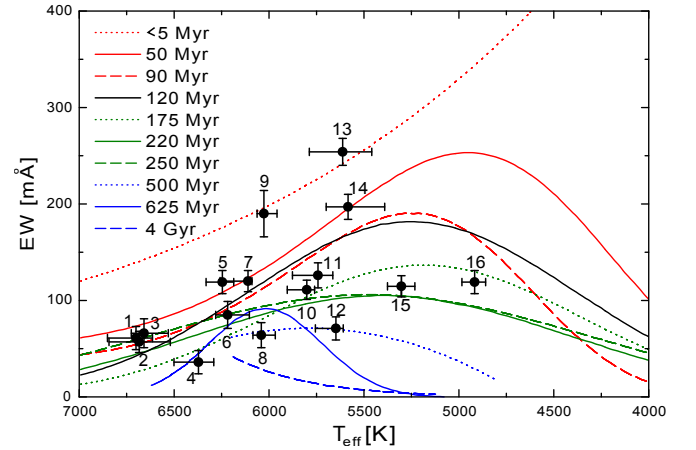


FIGURE 5 Lithium as age indicator for our 16 youngest FGKM stars. We show the equivalent widths of the Li (6708 Å) line dependant on the effective temperature for different ages, that are based on fits done by Eric Mamajek. The derived ages are given in Table 3.

6 | DISCUSSION

The aim of our project was to identify and/or confirm young mid- and late-type runaway stars from the catalogue by Tetzlaff et al. (2011) based on their location in the HRD with the more accurate *Gaia* DR2 data. In addition, we took spectra and searched for the absorption of the Li (6708 Å) line, which is a youth indicator. Our sample consists of 2 A-type, 38 F-type, 7 G-type and 4 K-type stars. Their SpT was assigned based on their T_{eff} with the SpT- $\log(T_{\text{eff}})$ -relation from Damiani et al. (2016).

We studied the surface gravity of our targets within the *StarHorse* catalogue to rule out possible sub-giants, that have typically $\log(g[\text{cm/s}^2]) < 3.8$. As a result of this, 23 targets could be excluded as already evolved stars.

The main goal of this study was to find stars that are younger or about 50 Myr. Therefore, we used isochrones, as illustrated in Fig. 3, to give an age limit of our identified dwarf stars. Due to their derived scatter of metallicity as explained above, assuming solar metallicity for our sample and using it

⁴<http://www.pas.rochester.edu/~emamajek/images/li.jpg>

TABLE 3 Our dwarf stars with their identification numbers as shown in Figure 3, Figure 4 and Figure 5, listed with their SpT derived from their T_{eff} using the SpT- $\log(T_{\text{eff}})$ -relation from Damiani et al. (2016), their distances d according to Bailer-Jones et al. (2018), the measured equivalent width of the Hydrogen Balmer line $EW_{\text{H}\alpha}$ (all in absorption) and the measured equivalent width of Li (6708 Å) EW_{Li} . Furthermore, we list the estimated age derived from the position in the HRD, as well as the age according to the lithium test from this work and the age from Tetzlaff et al. (2011).

id. nr.	Target	SpT *	d [pc] Bailer-Jones	$EW_{\text{H}\alpha}$ [mÅ] *	EW_{Li} [mÅ] *	age (HRD) [Myr] *	age (EW_{Li}) [Myr] *	age [Myr] Tetzlaff
	HIP 116983	A7 V	111 ± 1	1336 ± 21	-	$> 10, < 2000$	-	41.9 ± 19.1
	HIP 111647	A7 V	84.6 ± 0.4	1173 ± 21	-	$> 10, < 2000$	-	41.9 ± 32.4
	HIP 47725	F2 V	72.1 ± 0.2	1185 ± 19	-	$\geq 20, < 5000$	-	41.9 ± 31.9
1	HIP 28469	F2 V	91.1 ± 0.4	1332 ± 18	61 ± 12	≥ 10	$\leq 50 \dots 220$	-
	HIP 117835	F2 V	83.7 ± 0.3	1397 ± 19	-	$> 10, < 5000$	-	41.9 ± 32.4
2	HIP 113174	F2 V	42.8 ± 0.1	1317 ± 17	57 ± 11	$\geq 10, \leq 2000$	$\leq 50 \dots 220$	-
	HIP 25749	F2 V	55.1 ± 0.1	1249 ± 19	-	$> 10, < 5000$	-	41.9 ± 32.4
3	HIP 26690	F2 V	167 ± 2	1324 ± 22	66 ± 15	$> 5, < 10$	$\leq 50 \dots 220$	35.8 ± 21.9
	HIP 111446	F5 V	66.4 ± 0.4	1321 ± 19	-	$> 10, < 5000$	-	35.8 ± 8.8
	HIP 5913	F5 V	58.6 ± 0.2	1134 ± 18	-	$> 10, < 5000$	-	41.9 ± 32.4
	HIP 49700	F5 V	80.0 ± 0.4	1242 ± 14	-	$> 10, < 5000$	-	41.9 ± 32.4
	HIP 5081	F5 V	52.5 ± 0.4	$1038 \pm 20; 567 \pm 23^\dagger$	-	$> 5, < 10$	-	-
	HIP 57529	F5 V	92.5 ± 6.3	1133 ± 12	-	$> 5, < 20$	-	-
	HIP 35219	F5 V	52.2 ± 1.0	1134 ± 17	-	$> 10, < 5000$	-	-
4	HIP 2710	F6 V	40.6 ± 0.1	1344 ± 18	36 ± 12	$\geq 20, < 5000$	$175 \dots 625$	17.8 ± 5.6
5	HIP 22524	F6 V	50.4 ± 0.1	1225 ± 15	119 ± 12	$> 10, < 5000$	≤ 50	17.1 ± 3.0
6	HIP 54531	F6 V	61.0 ± 0.2	1065 ± 21	85 ± 14	$> 20, < 5000$	$90 \dots 625$	38.8 ± 22.9
7	HIP 51386	F8 V	31.0 ± 0.1	959 ± 14	120 ± 11	$> 20, < 5000$	$\leq 50 \dots 120$	25.5 ± 4.3
8	HIP 44212	F8 V	46.2 ± 0.1	1182 ± 19	64 ± 13	> 20	$175 \dots 500$	39.8 ± 4.6
9	HIP 30030	F8 V	51.9 ± 0.1	722 ± 30	190 ± 24	≥ 20	< 50	26.6 ± 5.3
10	HIP 114385	G0 V	30.3 ± 0.1	918 ± 14	111 ± 10	> 20	$175 \dots 250$	35.1 ± 10.5
11	HIP 115527	G0 V	30.4 ± 0.1	838 ± 16	126 ± 13	> 30	$90 \dots 175$	35.8 ± 9.7
12	HIP 19855	G2 V	22.1 ± 0.1	968 ± 15	71 ± 12	> 30	$500 \dots 625$	39.5 ± 17.4
13	HIP 16563	G2 V	36.4 ± 0.1	543 ± 18	254 ± 14	> 20	< 50	16.7 ± 1.1
14	HIP 71631	G5 V	34.4 ± 0.1	813 ± 20	197 ± 13	$\geq 20, \leq 30$	$\leq 50 \dots 90$	27.6 ± 4.2
15	HIP 7576	G8 V	24.0 ± 0.1	933 ± 12	114 ± 12	> 30	$220 \dots 250$	40.7 ± 7.9
	HIP 114379	K2 V	30.4 ± 0.1	$274 \pm 17; 43 \pm 8^\dagger$	-	$> 10, < 30$	-	23.9 ± 11.2
16	HIP 40774	K2 V	22.4 ± 0.1	703 ± 14	119 ± 12	> 40	~ 175	54.9 ± 10.4

* this work

† both H α -lines of this spectroscopic binary could be measured

for isochrone fitting seems reasonable. We considered possible multiplicity within our sample and checked the catalogue of Pourbaix et al. (2004) for spectroscopic binaries, to correct their position in the HRD. We list all identified binaries in Table 4 with their measured radial velocity, which was determined from the Ca (6718 Å) line. The secondary component of the double-lined binaries HIP 5081 and HIP 114379 could also be measured.

Nearly all dwarf stars are consistent within their uncertainties with isochrones in the range of a few Gyr. Therefore, another indicator is needed to confirm the youth of the targets. For this, we measured the equivalent width of the Li (6708 Å) line. HIP 16563 has the strongest lithium line with ($254 \pm$

14) mÅ. In contrast to this, 30 stars of the sample showed no significant Li (6708 Å) line within their spectra.

Equivalent width measurements of the dwarfs were then converted into abundances using the curves of growth from Soderblom et al. (1993). HIP 44212 is also listed in the catalogues of (Ramírez, Fish, Lambert, & Allende Prieto, 2012) and (Lambert & Reddy, 2004) and their measurements ($\log(N_{\text{Li}}) = 2.65 \pm 0.03$ and $\log(N_{\text{Li}}) = 2.55 \pm 0.10$, respectively) are consistent with our determined lithium abundance.

The dwarf stars were then compared to curves of clusters with known age as seen in Figure 5, based on their equivalent width of the Li (6708 Å) line and their effective temperature. These estimated ages from lithium measurements can be seen as upper limit and classify HIP 28469 (# 1), HIP 113174 (# 2),

HIP 26690 (#3), HIP 22524 (#5), HIP 51386 (#7), HIP 30030 (#9), HIP 16563 (#13) and HIP 71631 (#14) as young (≤ 50 Myr) according to Tetzlaff et al. (2011). For HIP 22524 (#5) we can derive an age > 10 Myr, < 5 Gyr from HRD isochrone fitting and ≤ 50 Myr from the lithium test. These ages are consistent with each other and also agree with the estimation of 17.1 ± 3.0 Myr from Tetzlaff et al. (2011), as given in Table 3.

For several targets, such as HIP 2710 (#4), HIP 44212 (#8), HIP 19855 (#12), HIP 7576 (#15) and HIP 40774 (#16), we could not confirm their ages from Tetzlaff et al. (2011), because they showed less lithium than we would expect for comparable stars with the same SpT. Within its 2σ uncertainty in Figure 5, HIP 44212 (#8) would cross the 4 Gyr curve and its age range would therefore be comparable with ages from Ramírez et al. (2012) ($4.98^{+1.15}_{-1.90}$ Gyr), Casagrande et al. (2011) ($3.78^{+3.12}_{-2.34}$ Gyr), Pace (2013) (3.91 ± 2.79 Gyr) and Mints & Hekker (2017) ($4.15^{+4.93}_{-2.25}$ Gyr). Additionally, this star is also located on the 5 Gyr isochrone in Figure 2. As counterparts to those mentioned stars, HIP 54531 (#6), HIP 114385 (#10) and HIP 115527 (#11) would just barely be, within their 2σ uncertainties, consistent with the young ages from Tetzlaff et al. (2011).

We found two young targets within our sample, namely HIP 30030 (#9) and HIP 16563 (#13), that show a relatively large amount of lithium in comparison to their expected lower age limit from their location in the HRD. Their spectra are given in Figure 6. These objects were assigned from HRD isochrone fitting to be ≥ 20 Myr and > 20 Myr, respectively. Their position in Figure 5 could suggest an age of ~ 5 Myr. However, these two stars should be handled with care, because as mentioned above the lithium method does not give very reliable age estimations below 20 Myr (Soderblom et al., 2014). Therefore, in combination with isochrone fitting and the lithium test, HIP 30030 (#9) is more likely older or equal than 20 Myr and younger than 50 Myr, while HIP 16563 (#13) is older than 20 Myr and younger than 50 Myr.

GJ 182 (HIP 23200) is one of the youngest stars (e.g. Bischoff, Mugrauer, Torres, et al., 2020) and, given its distance of 24.38 ± 0.02 pc (Bailer-Jones et al., 2018), there is no star known that is both younger and more nearby. Its age was estimated by Bischoff, Mugrauer, Torres, et al. (2020) to be ranging between 20 Myr and 50 Myr, which is consistent with ages from Brandt et al. (2017), Binks & Jeffries (2014) and Bell, Mamajek, & Naylor (2015) - and also with membership to the β Pic moving group (Lee & Song, 2018). HIP 113174 (#2) and HIP 51386 (#7) have comparable ages to GJ 182 and are not much further away than GJ 182 ($d \leq 2 \cdot d_{\text{GJ 182}}$, as listed in Table 3). Therefore, these two young runaway star candidates, which were listed as field stars in David & Hillenbrand (2015) and/or Pace (2013), are the best targets for

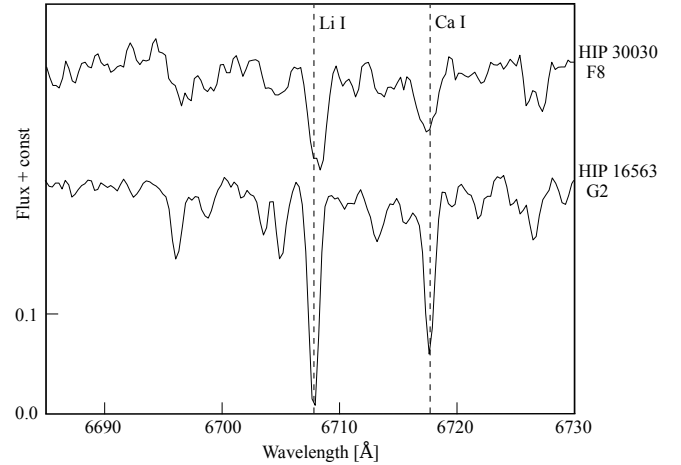


FIGURE 6 Spectra of HIP 30030 (#9) and HIP 16563 (#13).

follow-up investigations of their origin from either dynamical or supernova ejection based on their young age and proximity to the Earth. Even if HIP 26690 (#3) is further out, given its distance of 167 ± 2 pc (Bailer-Jones et al., 2018), it has a comparable age to HIP 113174 (#2) and HIP 51386 (#7) and is therefore also a good candidate. In contrast to the mentioned three targets, HIP 28469 (#1), HIP 22524 (#5), HIP 30030 (#9), HIP 16563 (#13) and HIP 71631 (#14) are rather no runaway stars, because they are associated with young nearby stellar clusters (Gagné et al., 2018; López-Santiago, Montes, Crespo-Chacón, & Fernández-Figueroa, 2006; Montes et al., 2001). HIP 28469 (#1) and HIP 22524 (#5) were assigned to be members of the Hyades cluster and HIP 30030 (#9) belongs to the Columba association (Gagné et al., 2018). Furthermore, HIP 16563 (#13) is part of the AB Doradus moving group (Gagné et al., 2018) and HIP 71631 (#14) is listed as member of the Local Association subgroup B4 in López-Santiago et al. (2006). As presented in Table 3, our derived age for HIP 30030 (#9) is consistent with 42^{+6}_{-4} Myr, the age of its associated cluster in Gagné et al. (2018). We derived an age of 20...50 Myr for HIP 16563 (#13), which younger than 149^{+51}_{-19} Myr of its moving group as given in Gagné et al. (2018). However, López-Santiago et al. (2006) list ages for the AB Doradus moving group ranging between 30 Myr and 150 Myr, which are consistent with our derived age for its possible member star HIP 16563 (#13). The Local Association subgroup B4 has an average age of ~ 150 Myr but also contains stars which are consistent with 80 Myr (López-Santiago et al., 2006). That fits with our derived age of 20...90 Myr for HIP 71631 (#14). The determined age of the stars in the Hyades cluster is 750 ± 100 Myr according to Gagné et al. (2018). However, the basis for the 625 Myr isochrone in Figure 5 is also the distribution of the Hyades

cluster. Those stars scatter around the 625 Myr isochrone in the original plot⁵, that was done by Eric Mamajek, and the location of the lithium richest members are consistent with the location of HIP 22524 (#5). HIP 28469 (#1) is also close to this area within its uncertainties. If HIP 28469 (#1) and HIP 22524 (#5) are actually members of the Hyades cluster, their upper age limit would be then the cluster age.

7 | CONCLUSIONS

We carried out spectroscopic follow-up observations for 51 targets from the catalogue by Tetzlaff et al. (2011) to search for the Li (6708 Å) absorption line, which is a youth indicator. 21 stars have a significantly detected lithium line within their spectra. In combination with isochrones based on the *Gaia* DR2, we classified 8 objects as young with ages ≤ 50 Myr. Some of these targets are already associated with young nearby stellar clusters. HIP 113174 (#2), HIP 26690 (#3) and HIP 51386 (#7) are the remaining young runaway star candidates, which are outside of known clusters. They are suitable for further follow-up observations to identify their place of origin and/or to search for possible companions.

As it is the standard in our survey the fully reduced FLECHAS spectra as well as the measured equivalent widths of the Li (6708 Å) line will be made available in *VizieR* after publication.

TABLE 4 Radial velocity measurements for the spectroscopic binaries as derived from the Ca (8500 Å) line and given with their Barycentric Julian Date (BJD).

Target	BJD	RV_1 [km/s]	RV_2 [km/s]
HIP 5081	2459061.55093	54.4 ± 4.0	-50.9 ± 4.1
HIP 22524	2458913.32631	32.2 ± 2.9	
HIP 26690	2458933.32562	19.4 ± 3.4	
HIP 64312	2458912.45917	-4.5 ± 3.3	
HIP 71631	2458927.37139	-22.2 ± 1.6	
HIP 82798	2458912.58774	-30.1 ± 3.0	
HIP 112821	2459044.49852	-4.4 ± 2.2	
HIP 114379	2459052.52385	15.7 ± 1.6	-32.5 ± 2.5

ACKNOWLEDGMENTS

We thank additional observers who have been involved in some of the observations of this project, obtained at the University

Observatory Jena and the Fred L. Whipple Observatory, in particular P. Berlind, S. Bischoff, M. Calkins, G. Esquerdo, L. Nueva and S. Quinn. This publication makes use of data products of the *VizieR* databases, operated at CDS, Strasbourg, France. We also thank the *Gaia* Data Processing and Analysis Consortium of the European Space Agency (ESA) for processing and providing the data of the *Gaia* mission.

We thank Eric Mamajek for providing the curves of lithium as age indicator for FGKM stars.

This work was supported by the Deutsche Forschungsgemeinschaft with financing the projects *NE 515/58-1* and *MU 2695/27-1*.

We thank the referee for helpful comments, which improved our manuscript.

How cite this article: Bischoff, R., Mugrauer, M., Torres, G. et al. (2021), Identification of additional young nearby runaway stars based on *Gaia* data release 2 observations and the lithium test, *Astron. Nachr.*, 2021

⁵<http://www.pas.rochester.edu/~emamajek/images/li.jpg>

APPENDIX A: ADDITIONAL TARGET INFORMATION

TABLE A1 Observation log. For each target we list the date and mid-time of the observation, as well as the individual exposure time (T_{exp}) of each FLECHAS spectrum and the signal-to-noise ratios (SNR) of the average of the three spectra, as measured at $\lambda = 6700 \text{ \AA}$.

Target	Date [UT]	T_{exp} [s]	SNR
HIP 1762	2020 Mar 23, 19:42	900	76
HIP 2710	2020 Sep 03, 01:02	450	101
HIP 5081	2020 Jul 31, 01:10	150	102
HIP 5913	2020 Mar 09, 21:10	900	93
HIP 7576	2020 Sep 03, 01:36	900	111
HIP 10141	2020 Mar 03, 23:16	600	78
HIP 11126	2020 Aug 05, 01:37	1200	87
HIP 11429	2020 Mar 04, 23:22	300	108
HIP 12083	2020 Mar 03, 22:16	600	98
HIP 12297	2020 Mar 21, 22:10	300	82
HIP 16563	2020 Mar 23, 20:36	900	91
HIP 19587	2020 Sep 03, 03:18	150	201
HIP 19855	2020 Mar 18, 19:23	450	103
HIP 22524	2020 Mar 04, 19:50	450	118
HIP 24817	2020 Mar 04, 19:32	150	160
HIP 25749	2020 Mar 04, 00:16	450	94
HIP 26690	2020 Mar 24, 19:50	1200	74
HIP 27841	2020 Mar 22, 20:16	600	76
HIP 28469	2020 Mar 18, 19:52	600	101
HIP 30030	2020 Mar 22, 19:32	900	50
HIP 35219	2020 Mar 03, 22:35	300	99
HIP 40774	2020 Mar 23, 21:42	1200	93
HIP 44212	2020 Mar 22, 21:31	900	87
HIP 47725	2020 Mar 21, 21:19	900	90
HIP 49700	2020 Mar 09, 23:18	900	121
HIP 51386	2020 Mar 04, 01:01	450	117
HIP 54531	2020 Mar 22, 22:42	1200	81
HIP 56770	2020 Mar 03, 21:14	150	123
HIP 57160	2020 Mar 10, 00:09	900	126
HIP 57529	2020 Mar 10, 01:19	600	126
HIP 64312	2020 Mar 03, 22:54	300	89
HIP 71631	2020 Mar 18, 20:52	600	90
HIP 74333	2020 Mar 04, 01:38	450	100
HIP 82798	2020 Mar 04, 02:06	300	102
HIP 89828	2020 Jul 30, 21:42	600	92
HIP 91594	2020 Mar 04, 04:35	450	84
HIP 103471	2020 Mar 04, 03:11	450	155
HIP 105607	2020 Jul 06, 22:47	300	83

Continued

Target	Date [UT]	T_{exp} [s]	SNR
HIP 106053	2020 Jul 06, 23:20	300	71
HIP 111446	2020 Jul 30, 02:05	600	91
HIP 111647	2020 Aug 07, 01:21	600	85
HIP 112821	2020 Jul 13, 23:54	600	83
HIP 113174	2020 Jul 06, 22:29	150	101
HIP 113811	2020 Jul 31, 00:33	900	121
HIP 113952	2020 Jul 22, 00:00	300	85
HIP 114379	2020 Jul 22, 00:32	900	124
HIP 114385	2000 Jul 21, 23:34	450	103
HIP 115527	2020 Aug 07, 02:21	600	91
HIP 115906	2020 Jul 31, 01:45	300	168
HIP 116983	2020 Jul 29, 23:42	1200	83
HIP 117835	2020 Jul 30, 00:59	900	89

TABLE A2 Measured equivalent widths (EW_{Li}) of the Li(6708 Å) line. Targets without significant detection ($EW_{\text{Li}} < 3 \cdot \sigma EW_{\text{Li}}$) are listed with "-".

Target	EW_{Li} [mÅ]	Target	EW_{Li} [mÅ]
HIP 1762	55 ± 14	HIP 54531	85 ± 14
HIP 2710	36 ± 12	HIP 56770	–
HIP 5081	–	HIP 57160	–
HIP 5913	–	HIP 57529	–
HIP 7576	114 ± 12	HIP 64312	–
HIP 10141	–	HIP 71631	197 ± 13
HIP 11126	–	HIP 74333	–
HIP 11429	–	HIP 82798	37 ± 11
HIP 12083	98 ± 12	HIP 89828	–
HIP 12297	–	HIP 91594	–
HIP 16563	254 ± 14	HIP 103471	95 ± 8
HIP 19587	–	HIP 105607	–
HIP 19855	71 ± 12	HIP 106053	76 ± 16
HIP 22524	119 ± 12	HIP 111446	–
HIP 24817	–	HIP 111647	–
HIP 25749	–	HIP 112821	–
HIP 26690	66 ± 15	HIP 113174	57 ± 11
HIP 27841	–	HIP 113811	–
HIP 28469	61 ± 12	HIP 113952	–
HIP 30030	190 ± 24	HIP 114379	–
HIP 35219	–	HIP 114385	111 ± 10
HIP 40774	119 ± 12	HIP 115527	126 ± 13
HIP 44212	64 ± 13	HIP 115906	–
HIP 47725	–	HIP 116983	–
HIP 49700	–	HIP 117835	–
HIP 51386	120 ± 11		

TABLE A3 Physical properties of the targets, namely the corrected apparent brightness G according to Maíz Apellániz & Weiler (2018), the effective temperature T_{eff} , stellar radius R , and luminosity L of the target stars (if available), from the *Gaia* DR2, as well as the derived extinction in the G -band A_G from Gontcharov & Mosenkov (2017). From these parameters together with the distances d by Bailer-Jones et al. (2018), the absolute G -band brightness M_G of the targets was calculated. The last column yields further remarks, with details listed in the footnote of this table.

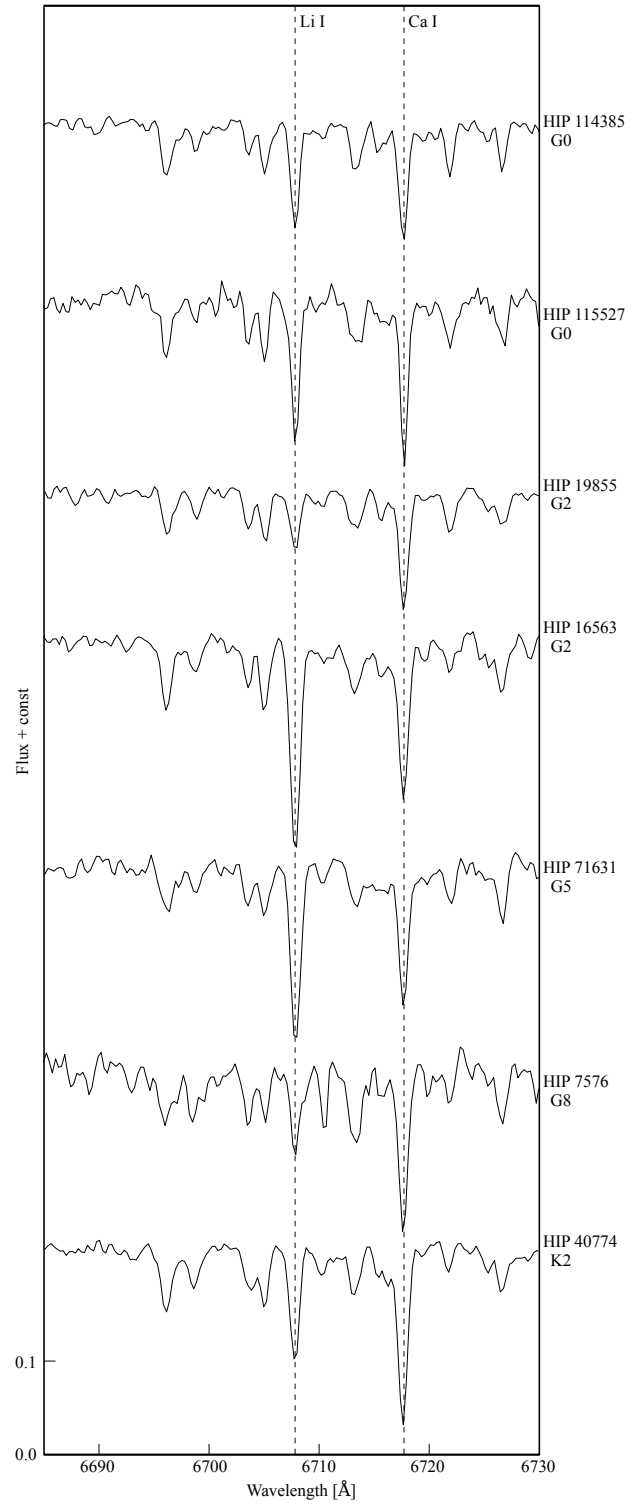
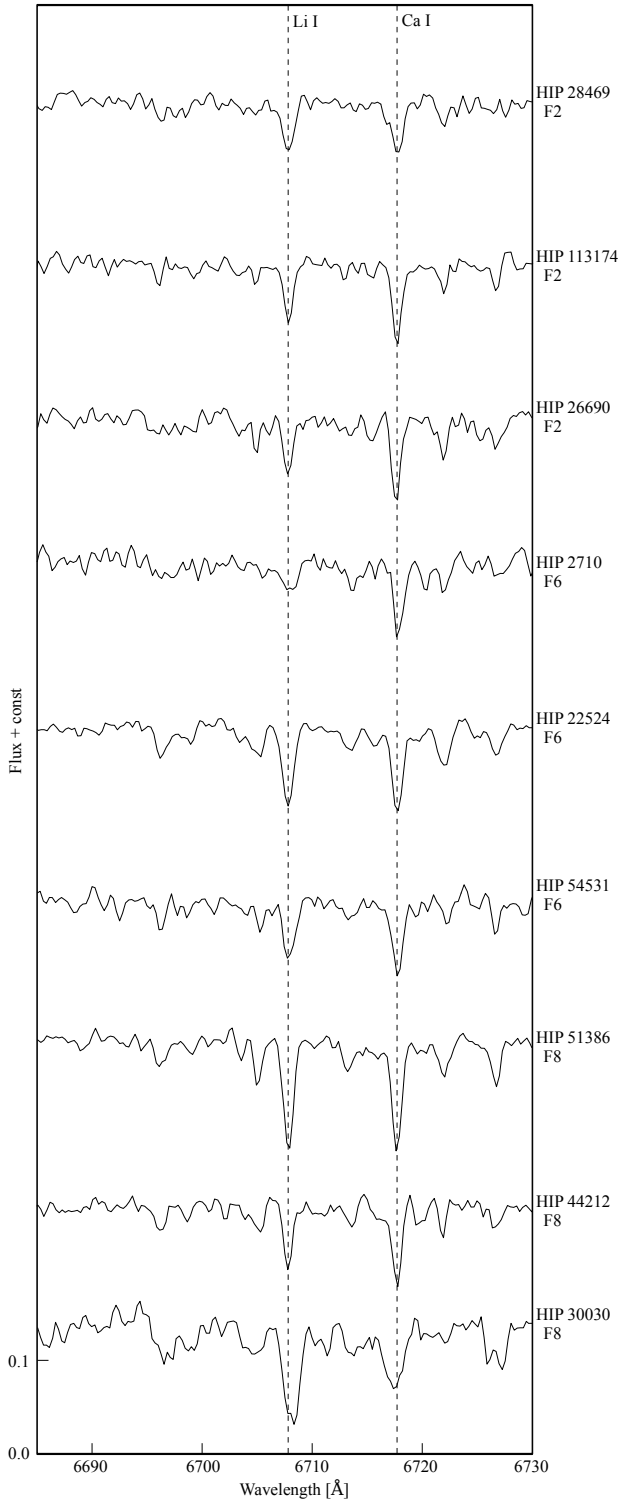
Target	d [pc]	G [mag]	A_G [mag]	M_G [mag]	T_{eff} [K]	R [R_{\odot}]	L [L_{\odot}]	rem.
HIP 1762	217^{+2}_{-2}	7.928 ± 0.001	$0.245^{+0.100}_{-0.099}$	$1.000^{+0.118}_{-0.120}$	6454^{+136}_{-116}	$3.86^{+0.15}_{-0.15}$	$23.3^{+0.3}_{-0.3}$	
HIP 2710	$40.6^{+0.1}_{-0.1}$	6.782 ± 0.001	$0.087^{+0.099}_{-0.087}$	$3.654^{+0.091}_{-0.104}$	6372^{+129}_{-81}	$1.25^{+0.03}_{-0.05}$	$2.33^{+0.01}_{-0.01}$	
HIP 5081	$52.5^{+0.4}_{-0.4}$	5.525 ± 0.002	$0.079^{+0.099}_{-0.079}$	$2.375^{+0.097}_{-0.117}$	6567^{+72}_{-104}	—	—	b
HIP 5913	$58.6^{+0.2}_{-0.2}$	7.202 ± 0.001	$0.126^{+0.099}_{-0.098}$	$3.236^{+0.104}_{-0.105}$	6605^{+134}_{-226}	$1.39^{+0.10}_{-0.06}$	$3.30^{+0.01}_{-0.01}$	
HIP 7576	$24.0^{+0.1}_{-0.1}$	7.442 ± 0.001	$0.047^{+0.099}_{-0.047}$	$5.491^{+0.050}_{-0.101}$	5303^{+73}_{-71}	$0.82^{+0.02}_{-0.03}$	$0.474^{+0.001}_{-0.001}$	
HIP 10141	$99.2^{+0.4}_{-0.4}$	6.559 ± 0.001	$0.150^{+0.099}_{-0.098}$	$1.428^{+0.107}_{-0.109}$	7077^{+165}_{-233}	$2.76^{+0.19}_{-0.12}$	$17.2^{+0.1}_{-0.1}$	
HIP 11126	180^{+2}_{-2}	8.056 ± 0.001	$0.205^{+0.100}_{-0.099}$	$1.574^{+0.119}_{-0.120}$	6380^{+122}_{-134}	$3.09^{+0.13}_{-0.12}$	$14.2^{+0.2}_{-0.2}$	
HIP 11429	$93.3^{+0.4}_{-0.4}$	7.341 ± 0.001	$0.134^{+0.099}_{-0.098}$	$2.357^{+0.108}_{-0.109}$	6716^{+46}_{-81}	$2.00^{+0.05}_{-0.02}$	$7.36^{+0.04}_{-0.04}$	
HIP 12083	197^{+1}_{-1}	6.529 ± 0.001	$0.260^{+0.100}_{-0.099}$	$-0.202^{+0.113}_{-0.114}$	6562^{+115}_{-103}	$6.46^{+0.21}_{-0.22}$	$69.8^{+0.7}_{-0.7}$	
HIP 12297	179^{+3}_{-2}	7.552 ± 0.001	$0.323^{+0.101}_{-0.099}$	$0.968^{+0.129}_{-0.131}$	6702^{+157}_{-167}	$3.50^{+0.18}_{-0.16}$	$22.3^{+0.4}_{-0.4}$	
HIP 16563	$36.4^{+0.1}_{-0.1}$	7.969 ± 0.002	$0.118^{+0.099}_{-0.098}$	$5.046^{+0.104}_{-0.106}$	5612^{+176}_{-153}	$0.85^{+0.05}_{-0.05}$	$0.645^{+0.002}_{-0.002}$	
HIP 19587	$36.5^{+0.6}_{-0.6}$	3.946 ± 0.003	$0.110^{+0.099}_{-0.098}$	$1.023^{+0.134}_{-0.136}$	6930^{+120}_{-320}	$3.62^{+0.35}_{-0.13}$	$27.2^{+0.5}_{-0.5}$	
HIP 19855	$22.1^{+0.1}_{-0.1}$	6.760 ± 0.001	$0.063^{+0.099}_{-0.063}$	$4.976^{+0.066}_{-0.102}$	5648^{+108}_{-39}	$0.89^{+0.01}_{-0.03}$	$0.724^{+0.001}_{-0.001}$	
HIP 22524	$50.4^{+0.1}_{-0.1}$	7.148 ± 0.001	$0.158^{+0.099}_{-0.098}$	$3.477^{+0.105}_{-0.379}$	6246^{+86}_{-60}	—	—	b
HIP 24817	$61.3^{+0.6}_{-0.6}$	5.232 ± 0.003	$0.181^{+0.100}_{-0.098}$	$1.112^{+0.121}_{-0.123}$	6602^{+97}_{-114}	$3.64^{+0.13}_{-0.11}$	$22.7^{+0.3}_{-0.3}$	
HIP 25749	$55.1^{+0.1}_{-0.1}$	7.026 ± 0.001	$0.134^{+0.099}_{-0.098}$	$3.185^{+0.103}_{-0.105}$	6663^{+80}_{-136}	$1.39^{+0.06}_{-0.03}$	$3.43^{+0.01}_{-0.01}$	
HIP 26690	167^{+2}_{-2}	8.302 ± 0.001	$0.237^{+0.100}_{-0.099}$	$2.555^{+0.171}_{-0.166}$	6659^{+67}_{-128}	—	—	b
HIP 27841	301^{+5}_{-5}	7.453 ± 0.001	$0.284^{+0.100}_{-0.099}$	$-0.222^{+0.132}_{-0.134}$	6166^{+139}_{-121}	$7.33^{+0.30}_{-0.32}$	$70.0^{+1.5}_{-1.5}$	
HIP 28469	$91.1^{+0.4}_{-0.4}$	7.400 ± 0.001	$0.166^{+0.100}_{-0.098}$	$2.436^{+0.108}_{-0.110}$	6701^{+150}_{-87}	$1.91^{+0.05}_{-0.08}$	$6.65^{+0.04}_{-0.04}$	
HIP 30030	$51.9^{+0.1}_{-0.1}$	7.697 ± 0.002	$0.213^{+0.100}_{-0.099}$	$3.906^{+0.107}_{-0.108}$	6027^{+36}_{-69}	$1.18^{+0.03}_{-0.01}$	$1.65^{+0.01}_{-0.01}$	
HIP 35219	$52.2^{+1.0}_{-1.0}$	6.628 ± 0.001	$0.174^{+0.100}_{-0.098}$	$2.866^{+0.139}_{-0.141}$	6511^{+79}_{-54}	$1.65^{+0.03}_{-0.03}$	$4.44^{+0.09}_{-0.09}$	
HIP 40774	$22.4^{+0.1}_{-0.1}$	8.069 ± 0.001	$0.071^{+0.099}_{-0.071}$	$6.249^{+0.081}_{-0.109}$	4917^{+67}_{-58}	$0.69^{+0.01}_{-0.02}$	$0.247^{+0.001}_{-0.001}$	
HIP 44212	$46.2^{+0.1}_{-0.1}$	7.646 ± 0.001	$0.166^{+0.100}_{-0.098}$	$4.158^{+0.104}_{-0.105}$	6041^{+44}_{-74}	$1.07^{+0.02}_{-0.02}$	$1.37^{+0.00}_{-0.00}$	
HIP 47725	$72.1^{+0.2}_{-0.2}$	7.590 ± 0.001	$0.047^{+0.099}_{-0.047}$	$3.252^{+0.054}_{-0.105}$	6762^{+307}_{-237}	$1.36^{+0.10}_{-0.11}$	$3.49^{+0.01}_{-0.01}$	
HIP 49700	$80.0^{+0.4}_{-0.4}$	7.708 ± 0.001	$0.095^{+0.099}_{-0.095}$	$3.097^{+0.105}_{-0.109}$	6575^{+152}_{-134}	$1.51^{+0.07}_{-0.06}$	$3.85^{+0.02}_{-0.02}$	
HIP 51386	$31.0^{+0.1}_{-0.1}$	6.711 ± 0.001	$0.055^{+0.099}_{-0.055}$	$4.198^{+0.062}_{-0.106}$	6111^{+147}_{-21}	$1.08^{+0.00}_{-0.05}$	$1.46^{+0.01}_{-0.00}$	
HIP 54531	$61.0^{+0.2}_{-0.2}$	8.104 ± 0.001	$0.095^{+0.099}_{-0.095}$	$4.082^{+0.103}_{-0.107}$	6218^{+63}_{-114}	$1.08^{+0.04}_{-0.03}$	$1.56^{+0.01}_{-0.01}$	
HIP 56770	$47.8^{+0.5}_{-0.5}$	5.459 ± 0.002	$0.008^{+0.099}_{-0.008}$	$2.054^{+0.033}_{-0.124}$	6934^{+74}_{-156}	$2.31^{+0.11}_{-0.05}$	$11.1^{+0.1}_{-0.1}$	
HIP 57160	147^{+1}_{-1}	7.579 ± 0.001	$0.087^{+0.099}_{-0.087}$	$1.657^{+0.100}_{-0.113}$	6830^{+127}_{-260}	$2.74^{+0.22}_{-0.10}$	$14.7^{+0.1}_{-0.1}$	
HIP 57529	$92.5^{+6.3}_{-5.6}$	7.204 ± 0.005	$0.047^{+0.099}_{-0.047}$	$2.326^{+0.186}_{-0.246}$	6531^{+154}_{-218}	—	—	a
HIP 64312	156^{+4}_{-3}	6.724 ± 0.001	$0.189^{+0.100}_{-0.098}$	$0.805^{+0.148}_{-0.150}$	6742^{+174}_{-87}	—	—	b
HIP 71631	$34.4^{+0.1}_{-0.1}$	7.492 ± 0.001	$0.039^{+0.099}_{-0.039}$	$4.843^{+0.115}_{-0.118}$	5584^{+115}_{-193}	—	—	b
HIP 74333	155^{+1}_{-1}	7.060 ± 0.001	$0.118^{+0.099}_{-0.098}$	$0.990^{+0.114}_{-0.116}$	7089^{+211}_{-81}	$3.42^{+0.08}_{-0.20}$	$26.6^{+0.3}_{-0.3}$	
HIP 82798	$75.4^{+0.3}_{-0.3}$	6.260 ± 0.001	$0.181^{+0.100}_{-0.098}$	$1.691^{+0.107}_{-0.380}$	7100^{+160}_{-124}	—	—	b
HIP 89828	$98.8^{+0.6}_{-0.6}$	7.231 ± 0.001	$0.395^{+0.101}_{-0.100}$	$1.861^{+0.113}_{-0.115}$	6060^{+364}_{-177}	$2.75^{+0.17}_{-0.30}$	$9.22^{+0.07}_{-0.07}$	
HIP 91594	133^{+2}_{-2}	7.124 ± 0.001	$0.402^{+0.101}_{-0.100}$	$1.103^{+0.130}_{-0.131}$	6911^{+335}_{-346}	$2.99^{+0.32}_{-0.27}$	$18.3^{+0.3}_{-0.3}$	
HIP 103471	185^{+1}_{-1}	7.180 ± 0.001	$0.142^{+0.099}_{-0.098}$	$0.707^{+0.112}_{-0.113}$	7007^{+144}_{-263}	$3.94^{+0.31}_{-0.15}$	$33.7^{+0.3}_{-0.3}$	
HIP 105607	109^{+1}_{-1}	6.421 ± 0.001	$0.197^{+0.100}_{-0.098}$	$1.044^{+0.119}_{-0.120}$	6241^{+16}_{-47}	$4.14^{+0.06}_{-0.02}$	$23.4^{+0.1}_{-0.1}$	
HIP 106053	105^{+11}_{-9}	6.546 ± 0.008	$0.118^{+0.099}_{-0.098}$	$1.320^{+0.305}_{-0.326}$	6531^{+154}_{-218}	—	—	a
HIP 111446	$66.4^{+0.4}_{-0.4}$	7.487 ± 0.001	$0.110^{+0.099}_{-0.098}$	$3.265^{+0.112}_{-0.113}$	6640^{+175}_{-148}	$1.36^{+0.07}_{-0.07}$	$3.25^{+0.02}_{-0.02}$	
HIP 111647	$84.6^{+0.4}_{-0.4}$	7.381 ± 0.003	$0.118^{+0.099}_{-0.098}$	$2.626^{+0.110}_{-0.111}$	7100^{+213}_{-144}	$1.60^{+0.07}_{-0.09}$	$5.86^{+0.04}_{-0.04}$	
HIP 112821	101^{+1}_{-1}	7.294 ± 0.001	$0.095^{+0.099}_{-0.095}$	$2.180^{+0.106}_{-0.380}$	5728^{+92}_{-128}	—	—	b
HIP 113174	$42.8^{+0.1}_{-0.1}$	5.799 ± 0.001	$0.095^{+0.099}_{-0.095}$	$2.549^{+0.101}_{-0.105}$	6684^{+159}_{-164}	$1.89^{+0.10}_{-0.09}$	$6.43^{+0.02}_{-0.02}$	

Continued

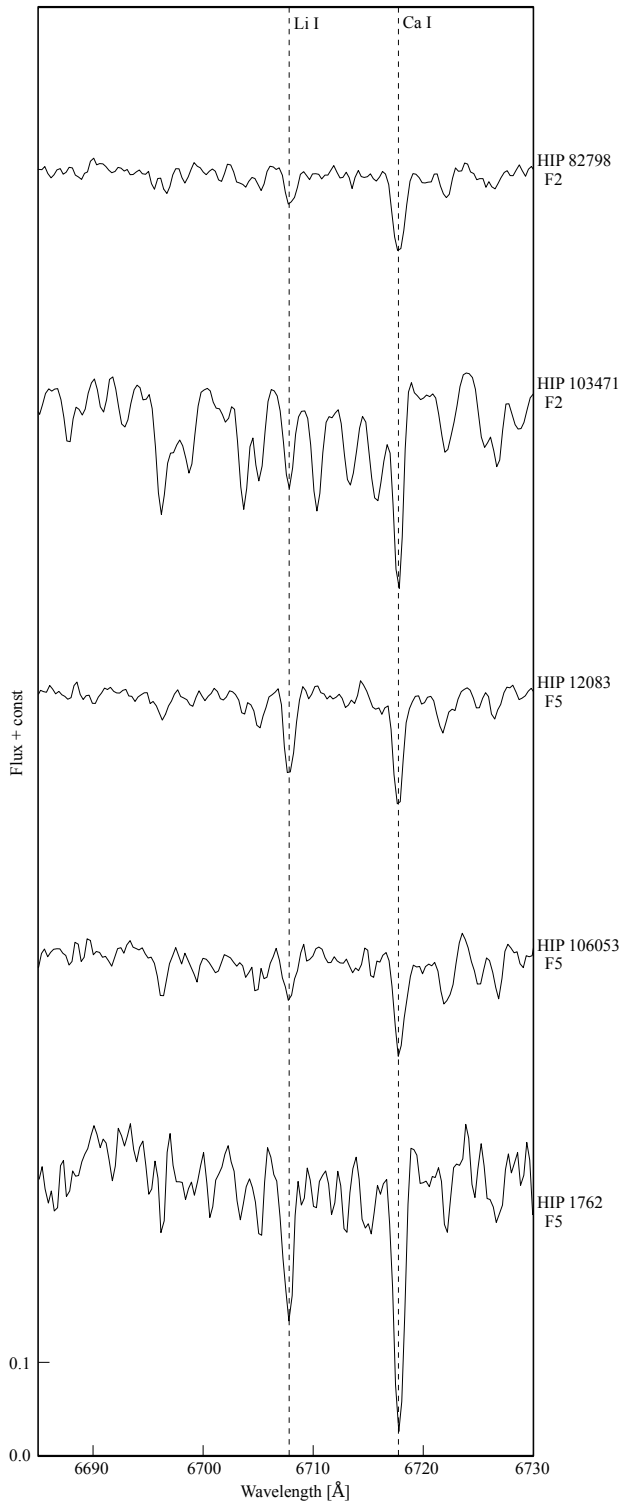
Target	d [pc]	G [mag]	A_G [mag]	M_G [mag]	T_{eff} [K]	R [R_{\odot}]	L [L_{\odot}]	rem.
HIP 113811	676^{+2027}_{-290}	7.405 ± 0.011	$0.147^{+0.049}_{-0.049}$	$-1.891^{+1.275}_{-3.070}$	4457^{+297}_{-161}	—	—	a c
HIP 113952	$72.1^{+0.2}_{-0.2}$	6.651 ± 0.001	$0.103^{+0.099}_{-0.098}$	$2.260^{+0.105}_{-0.106}$	6680^{+301}_{-112}	$2.15^{+0.07}_{-0.18}$	$8.30^{+0.04}_{-0.04}$	
HIP 114379	$30.4^{+0.1}_{-0.1}$	7.653 ± 0.001	$0.079^{+0.099}_{-0.079}$	$5.845^{+0.087}_{-0.107}$	4979^{+169}_{-106}	—	—	b
HIP 114385	$30.3^{+0.1}_{-0.1}$	6.980 ± 0.001	$0.079^{+0.099}_{-0.079}$	$4.493^{+0.086}_{-0.106}$	5801^{+103}_{-41}	$1.04^{+0.01}_{-0.04}$	$1.10^{+0.01}_{-0.01}$	
HIP 115527	$30.4^{+0.1}_{-0.1}$	7.432 ± 0.001	$0.071^{+0.099}_{-0.071}$	$4.945^{+0.077}_{-0.105}$	5742^{+135}_{-78}	$0.87^{+0.02}_{-0.04}$	$0.734^{+0.002}_{-0.003}$	
HIP 115906	287^{+62}_{-43}	5.680 ± 0.005	$0.142^{+0.099}_{-0.098}$	$-1.754^{+0.459}_{-0.531}$	4853^{+235}_{-297}	—	—	a
HIP 116983	111^{+1}_{-1}	8.237 ± 0.001	$0.071^{+0.099}_{-0.071}$	$2.932^{+0.083}_{-0.111}$	7163^{+233}_{-253}	$1.40^{+0.10}_{-0.09}$	$4.62^{+0.04}_{-0.03}$	
HIP 117835	$83.7^{+0.3}_{-0.3}$	7.903 ± 0.001	$0.055^{+0.099}_{-0.055}$	$3.235^{+0.064}_{-0.107}$	6694^{+213}_{-169}	$1.39^{+0.08}_{-0.08}$	$3.52^{+0.02}_{-0.02}$	

- a - *Hipparcos* parallax (van Leeuwen, 2007) was used for distance determination, H_p and $V - I$ magnitudes from *Hipparcos* (Perryman et al., 1997) were transformed into G -band magnitude according to Evans et al. (2018), T_{eff} (Damiani et al., 2016) according to the *Hipparcos* spectral type
- b - spectroscopic binary (M_G therefore up to ~ 0.75 mag fainter as expected from *Gaia* DR2 entry)
- c - $E(g - r)$ from Green et al. (2019) was converted into A_G according to Wang & Chen (2019)

APPENDIX B: DWARF STARS WITH SIGNIFICANT LITHIUM DETECTION



APPENDIX C: SUB-GIANT/GIANT STARS WITH SIGNIFICANT LITHIUM DETECTION



REFERENCES

- Anders, F., Khalatyan, A., Chiappini, C. et al. 2019, August, *A&A*, 628, A94.
- Andrae, R., Fouesneau, M., Creevey, O. et al. 2018, Aug, *A&A*, 616, A8.
- Bailer-Jones, C. A. L., Rybizki, J., Fouesneau, M., Mantelet, G., & Andrae, R. 2018, Aug, *AJ*, 156(2), 58.
- Baraffe, I., Homeier, D., Allard, F., & Chabrier, G. 2015, May, *A&A*, 577, A42.
- Bell, C. P. M., Mamajek, E. E., & Naylor, T. 2015, Nov, *MNRAS*, 454(1), 593-614.
- Binks, A. S., & Jeffries, R. D. 2014, Feb, *MNRAS*, 438(1), L11-L15.
- Bischoff, R., Mugrauer, M., Lux, O., Zehe, T., Heyne, T., Wagner, D., & Geymeier, M. 2020, December, *Astronomische Nachrichten*, 341(10), 989-995.
- Bischoff, R., Mugrauer, M., Torres, G. et al. 2020, November, *Astronomische Nachrichten*, 341(9), 908-942.
- Bischoff, R., Mugrauer, M., Zehe, T. et al. 2017, Jul, *Astronomische Nachrichten*, 338(6), 671-679.
- Blaauw, A. 1961, May, *Bull. Astron. Inst. Netherlands*, 15, 265.
- Brandt, T. D., McElwain, M. W., Turner, E. L. et al. 2017, May, *VizieR Online Data Catalog*, JApJ/794/159.
- Bressan, A., Marigo, P., Girardi, L., Salasnich, B., Dal Cero, C., Rubele, S., & Nanni, A. 2012, November, *MNRAS*, 427(1), 127-145.
- Brewer, J. M., Fischer, D. A., Valenti, J. A., & Piskunov, N. 2016, August, *ApJS*, 225(2), 32.
- Casagrande, L., Schönrich, R., Asplund, M. et al. 2011, June, *A&A*, 530, A138.
- Casamiquela, L., Tarricq, Y., Soubiran, C., Blanco-Cuaresma, S., Jofré, P., Heiter, U., & Tucci Maia, M. 2020, March, *A&A*, 635, A8.
- Coluzzi, R. 1993, Jul, *Bulletin d'Information du Centre de Donnees Stellaires*, 43, 7.
- Damiani, C., Meunier, J. C., Moutou, C., Deleuil, M., Ysard, N., Baudin, F., & Deeg, H. 2016, Nov, *A&A*, 595, A95.
- David, T. J., & Hillenbrand, L. A. 2015, May, *ApJ*, 804(2), 146. doi: Escorza, A., Karinkuzhi, D., Jorissen, A. et al. 2019, June, *A&A*, 626, A128.
- Evans, D. W., Riello, M., De Angeli, F. et al. 2018, August, *A&A*, 616, A4.
- Fekel, F. C., Henry, G. W., & Tomkin, J. 2017, September, *AJ*, 154(3), 120.
- Fűrész, G. 2008. (PhD dissertation). University of Szeged, Hungary.
- Franchini, M., Morossi, C., di Marcantonio, P., Malagnini, M. L., & Chavez, M. 2014, July, *MNRAS*, 442(1), 220-228.
- Gagné, J., Mamajek, E. E., Malo, L. et al. 2018, March, *ApJ*, 856(1), 23.
- Gaia Collaboration, Brown, A. G. A., Vallenari, A. et al. 2018, Aug, *A&A*, 616, A1.
- Gontcharov, G. A., & Mosenkov, A. V. 2017, December, *MNRAS*, 472(4), 3805-3820.
- Gray, R. O., Corbally, C. J., Garrison, R. F. et al. 2006, July, *AJ*, 132(1), 161-170.
- Gray, R. O., Corbally, C. J., Garrison, R. F., McFadden, M. T., & Robinson, P. E. 2003, October, *AJ*, 126(4), 2048-2059.
- Green, G. M., Schlafly, E., Zucker, C., Speagle, J. S., & Finkbeiner, D. 2019, December, *ApJ*, 887(1), 93.
- Griffin, R. F. 2001, June, *The Observatory*, 121, 162-171.
- Heyne, T., Mugrauer, M., Bischoff, R. et al. 2020, January, *Astronomische Nachrichten*, 341(1), 99-117.
- Irrgang, A., Desphande, A., Moehler, S., Mugrauer, M., & Janousch,

- D. 2016, Jun, *A&A*, 591, L6.
- König, B., Guenther, E. W., Woitas, J., & Hatzes, A. P. 2005, May, *A&A*, 435(1), 215-223.
- Kunder, A., Kordopatis, G., Steinmetz, M. et al. 2017, February, *AJ*, 153(2), 75.
- Lambert, D. L., & Reddy, B. E. 2004, April, *MNRAS*, 349(2), 757-767. doi:
- Lee, J., & Song, I. 2018, April, *MNRAS*, 475(3), 2955-2970.
- López-Santiago, J., Montes, D., Crespo-Chacón, I., & Fernández-Figueroa, M. J. 2006, June, *ApJ*, 643(2), 1160-1165.
- Luck, R. E. 2017, January, *AJ*, 153(1), 21.
- Maíz Apellániz, J., & Weiler, M. 2018, November, *A&A*, 619, A180. doi:
- Mann, A. W., Brewer, J. M., Gaidos, E., Lépine, S., & Hilton, E. J. 2013, February, *AJ*, 145(2), 52.
- Marsden, S. C., Petit, P., Jeffers, S. V. et al. 2014, November, *MNRAS*, 444(4), 3517-3536.
- Mints, A., & Hekker, S. 2017, August, *A&A*, 604, A108. doi:
- Montes, D., López-Santiago, J., Gálvez, M. C., Fernández-Figueroa, M. J., De Castro, E., & Cornide, M. 2001, November, *MNRAS*, 328(1), 45-63.
- Mugrauer, M., Avila, G., & Guirao, C. 2014, Jan, *Astronomische Nachrichten*, 335(4), 417.
- Neuhäuser, R. 1997, Jan, *Science*, 276, 1363-1370.
- Nordstrom, B., Stefanik, R. P., Latham, D. W., & Andersen, J. 1997, November, *A&AS*, 126, 21-30.
- Ochsenbein, F., Bauer, P., & Marcout, J. 2000, Apr, *A&AS*, 143, 23-32.
- Pace, G. 2013, March, *A&A*, 551, L8. doi:
- Pecaut, M. J., & Mamajek, E. E. 2013, September, *ApJS*, 208(1), 9.
- Perryman, M. A. C., Lindegren, L., Kovalevsky, J. et al. 1997, Jul, *A&A*, 500, 501-504.
- Petigura, E. A., & Marcy, G. W. 2011, July, *ApJ*, 735(1), 41.
- Pfau, W. 1984, Jan, *Jenaer Rundschau*, 29(3), 121-122.
- Pourbaix, D., Tokovinin, A. A., Batten, A. H. et al. 2004, September, *A&A*, 424, 727-732.
- Poveda, A., Ruiz, J., & Allen, C. 1967, Apr, *Boletín de los Observatorios Tonantzintla y Tacubaya*, 4, 86-90.
- Ramírez, I., Fish, J. R., Lambert, D. L., & Allende Prieto, C. 2012, September, *ApJ*, 756(1), 46.
- Salaris, M., & Cassisi, S. 2005, Evolution of Stars and Stellar Populations.
- Soderblom, D. R., Hillenbrand, L. A., Jeffries, R. D., Mamajek, E. E., & Naylor, T. 2014, January, Ages of Young Stars. H. Beuther, R. S. Klessen, C. P. Dullemond, et al. (Eds.), Protostars and Planets VI p. 219.
- Soderblom, D. R., Jones, B. F., Balachandran, S., Stauffer, J. R., Duncan, D. K., Fedele, S. B., & Hudon, J. D. 1993, September, *AJ*, 106, 1059.
- Stassun, K. G., Oelkers, R. J., Paegert, M. et al. 2019, October, *AJ*, 158(4), 138.
- Szentgyorgyi, A. H., & Furész, G. 2007, Jun, Precision Radial Velocities for the Kepler Era. S. Kurtz (Ed.), Revista Mexicana de Astronomia y Astrofisica Conference Series Vol. 28, p. 129-133.
- Tetzlaff, N., Neuhäuser, R., & Hohle, M. M. 2011, Jan, *MNRAS*, 410(1), 190-200.
- Tody, D. 1993, January, IRAF in the Nineties. R. J. Hanisch, R. J. V. Brissenden, & J. Barnes (Eds.), Astronomical Data Analysis Software and Systems II Vol. 52, p. 173.
- Valenti, J. A., & Fischer, D. A. 2005, July, *ApJS*, 159(1), 141-166.
- van Leeuwen, F. 2007, Nov, *A&A*, 474(2), 653-664.
- Wang, S., & Chen, X. 2019, June, *ApJ*, 877(2), 116.
- Weiler, M. 2018, October, *A&A*, 617, A138. doi:

How cite this article: Bischoff, R., Mugrauer, M., Torres, G. et al. (2021), Identification of additional young nearby runaway stars based on Gaia data release 2 observations and the lithium test, *Astron. Nachr.*, 2021

AUTHOR BIOGRAPHY

Richard Bischoff is a PhD student at the Astrophysical Institute and University Observatory Jena. His main field of research are photometry and spectroscopy of exoplanet candidate host stars.